X-ray imaging of water flow through soil

Lorenzo Garbari

Degree project • 30 hp
Swedish University of Agricultural Sciences, SLU
Faculty of natural resources and agricoltural sciences
Soil science
Soil water and environment
2020

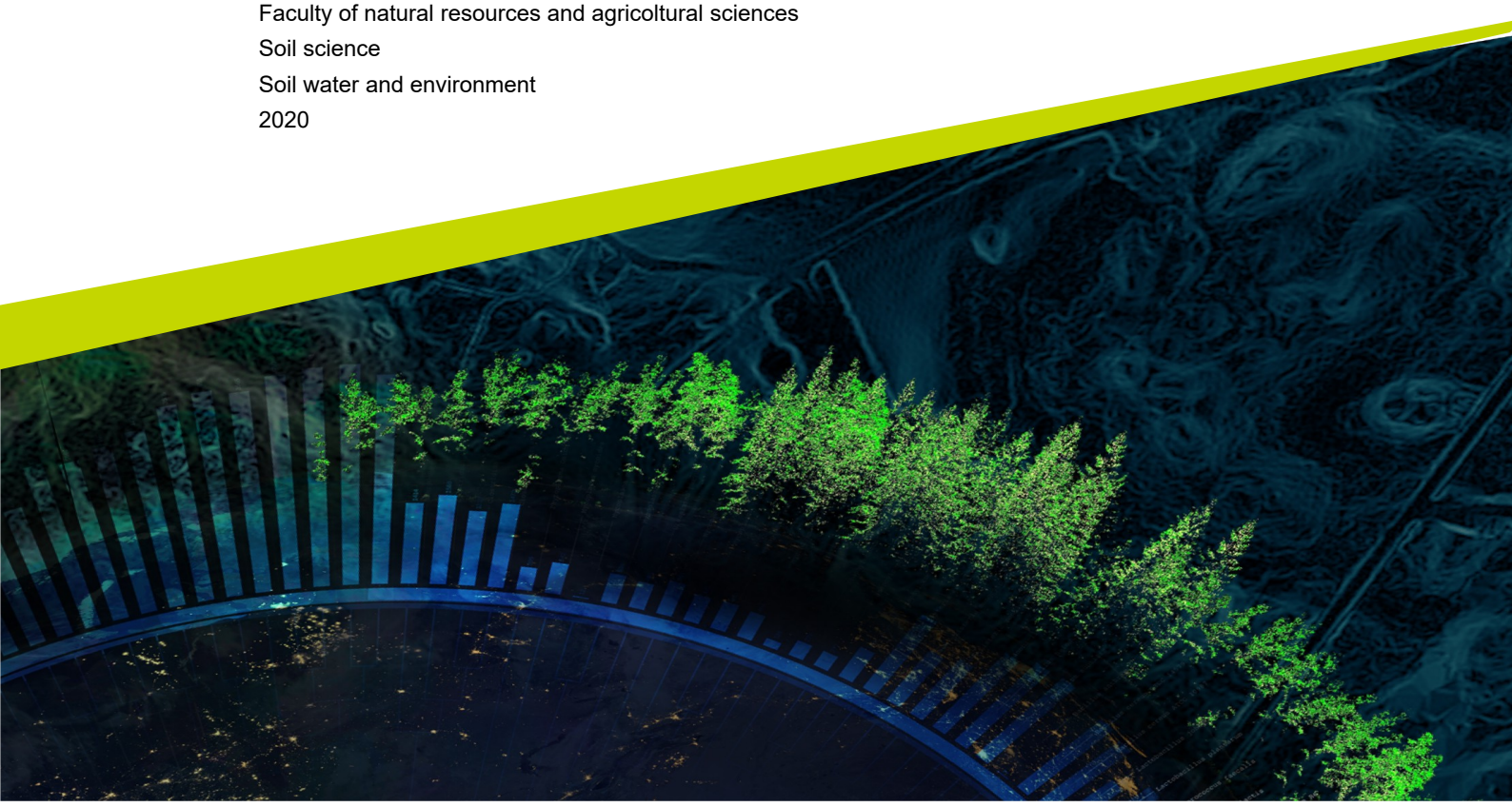

X-ray imaging of water flow through soil

Lorenzo Garbari

Supervisor:	**Johannes Koestel, SLU, soil and environment**
Assistant supervisor:	Daniel Iseskog, SLU, Soil Mechanics and Soil Management Gloria Falsone,
Assistant supervisor:	università di Bologna, DISTAL
Examiner:	Nicholas Jarvis, SLU, soil and environment

Credits:	30 hp
Level:	A2E
Course title:	**Degree project**
Course code:	**EX0880**
Programme/education:	**Soil water and environment**
Course coordinating dept:	
Place of publication:	**SLU**
Year of publication:	**2020**
Cover picture:	
Title of series:	
Part number: 2020:23	
ISSN:	

Keywords:
Infiltration, tomography, soil structure, soil porosity, wetting front, x-ray

Swedish University of Agricultural Sciences
Faculty of natural resources and agricoltural sciences
Department of soil and environment

Contents

1 Introduction **1**

1.1 Water infiltration into soil: a state of the art 1

1.1.1 Soil structure 2

1.1.2 Study scales 2

1.1.3 Uniform and non-uniform flow 3

1.1.4 Macropore flow and funnel flow 4

1.1.5 Finger flow 5

1.1.6 Water repellent soils 6

1.1.7 Antecedent soil moisture 7

1.2 X-ray imaging 8

1.3 Aim 9

2 Material and methods **10**

2.1 Experimental set up 10

2.2 Box design 10

2.3 Irrigation device 11

2.4 Implementation of the set up 12

2.5 Set up testing and optimization 13

2.6 Sample preparation 14

2.7 Irrigation experiments 15

2.8 X-ray imaging 15

2.9 Images of the 3D soil structure 16

2.10 Wetting front images 17

2.10.1 Image preparation 17

2.10.2 Image segmentation 18

2.10.2.1 2D images 18

2.10.2.2 3D images 18

2.10.3 Image analysis 18

3 Results and discussion **21**

3.1 Soil structure and macroporosity 21

3.2 Wetting fronts comparison 21
3.3 Average infiltration velocity 24
3.4 Water repellency 26
3.5 Wetting front tortuosity 26
3.6 Samples structure changes 29
3.7 Weaknesses of the set up 30

4 Conclusions **32**

1 Introduction

Water is one of the most valuable resources of our planet and because of that it is very important to know and comprehend every step of its cycle. This thesis focuses on one of these steps: water flow through soil. A good understanding of how water flows through soil is crucial to be able to comprehend other processes that are related to it like pollutants transport, soil erosion, recharge of groundwater, etc. The way water flows through the soil depends on many factors. The ones investigated in this thesis are soil structure, irrigation intensity, water repellency and antecedent soil moisture. It has always been just assumed that if an irrigation is repeated on the same soil the infiltration pattern would remain the same, this study aims to fill that knowledge gap.

The approach used in this study helps to better understand how water flow through soil and, indirectly, solute transport. Clothier et al. (2008) pointed up very well how important is the role played by preferential flow and transport in many ecosystem services. Ecosystem services are all the benefits provided by the ecosystems to the human population (Costanza et al., 1997). Clothier et al. (2008) deemed that preferential flow and transport influence fifteen of the seventeen ecosystem services analysed by Costanza et al. (1997), twelve of which are influenced positively while three negatively. They estimated, starting from the results of Costanza et al. (1997) that the effects of preferential flow and transport on the ecosistems are globally worth 304 billion of US dollars. This underlines how important it is to understand at the maximum of our capabilities how preferential flow works in order to enhance its good effects and minimize the bad ones. I like to think that this thesis will help to do a little step forward the achievement of this goal.

1.1 Water infiltration into soil: a state of the art

Infiltration is the process that characterizes water entry into the soil. The soil infiltrability is the maximum volume of water infiltrating through the soil per unit area in a certain amount of time (Parr et al., 1960). Soil infiltrability depends on different factors (Lili et al., 2008): (a) soil texture and structure, presence of macropores and in general a high soil porosity eases the infiltration process; (b) soil water content, the lower it is the higher the infiltration rate will be; (c) time, usually soil infiltrability is high at the beginning of an infiltration event but decreases over time; and (d) irrigation rate (or rainfall intensity),

if it is lower than the infiltrability the infiltration process is controlled by the irrigation rate otherwise it will be controlled by the infitrability.

1.1.1 Soil structure

There is no universally accepted way to measure soil structure (Díaz-Zorita et al., 2002; Hillel, 2003). Soil structure describes the aggregation of soil particles and the consequent pore distribution without taking into consideration the chemical characteristics of the solid phase (Rabot et al., 2018). According to this definition soil structure should be analysed from both, solid phase and pore perspectives.

The solid phase perspective divides soil solids into three classes: (a) primary particles; (b) microaggregates; (c) macroaggregates.

According to Pagliai et al. (2004) the pore space is very important for many processes in soils. Pores, like aggregates, can be divided into (a) micropores, (b) mesopores and (c) macropores. There are no official thresholds between these catecories (Rabot et al., 2018). Among these pore classes, the one that is mostly related to preferential flow is the macropores class. Macropores can be distinguished into four types (Hillel, 2003): (a) pores formed by burrowing animals, which are usually cylindrical and their diameter can measure up to 50 mm, (b) pores formed by plants roots that are tubular as well and their size depends on the plant, (c) cracks and fissures, these are formed by physical processes like swelling-and-shrinking and freezing-and-thawing and (d) natural soil pipes, that can be formed by internal erosion exerted by subsurface flows.

1.1.2 Study scales

Studies on water flow through soil have to be done in different ways depending on the scale of it. There are studies regarding water flow at pore scale, Darcian scale and areal scale. Pore scale studies concern preferential flow through pores and fractures while studies at the Darcian scale focuse on unstable and funnel flow caused by (a) layers in the soil profiles, (b) water repellency, (c) stones or macroaggregates and (d) changes of the hydraulic properties of the soil (Hendricks et al., 2001). The main differences between pore and Darcian scale are summarized in Table1 and in Figure1.

Table 1: Main characteristics of preferential flow at pore and Darcian scale. (Table taken from Hendricks et al. (2001) and modified)

Pore and Darcian scales			
Spatial scale	Domain	Critical parameters	Scale
Pore	Macropores, Fractures	Macropores Fracture width	Seconds Minutes Days
Darcian	Laboratory, Soil Profiles	Hydraulic Properties	Minutes Hours Months

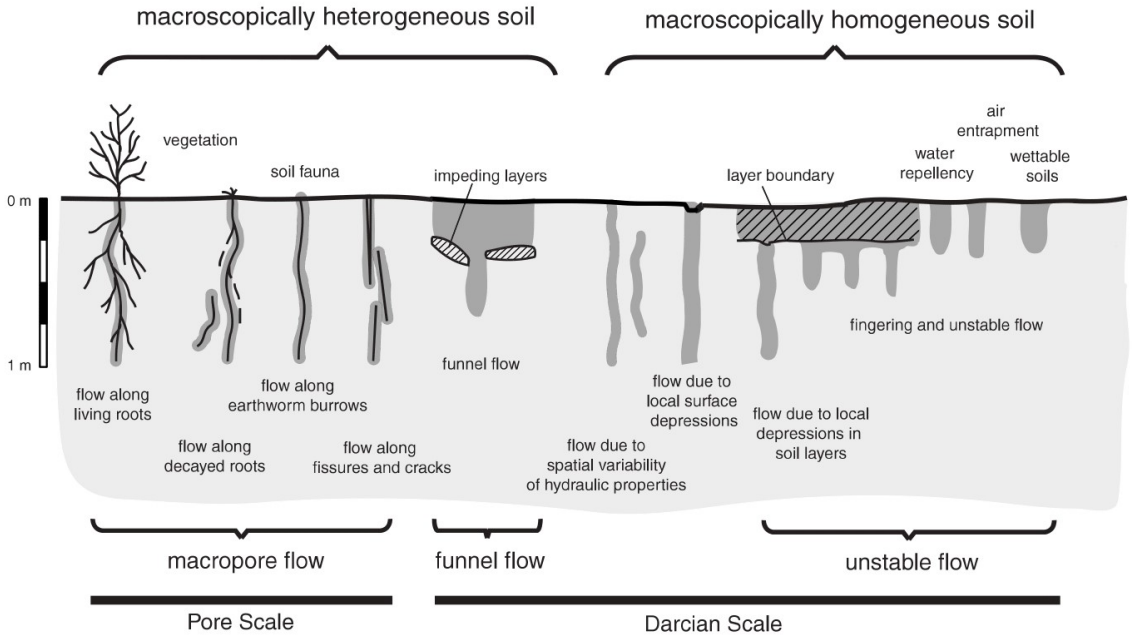

Figure 1: Different preferential flow mechanisms observed at pore and Darcian scales. Picture taken from Hendricks et al. (2001)

1.1.3 Uniform and non-uniform flow

There are different ways for water to flow through the soil. A first distinction can be made between uniform flow and non-uniform flow (Hendricks et al., 2001): (a) uniform flow is rarely observed in nature and most likely occurs in soils with an homogeneus structure.

It refers to a wetting front that is always parallel to the soil surface, it is very unlikely to happen under field conditions because there are so many factors that can trigger non-uniform flow. (b) Non-uniform flow, also called preferential flow, is characterized by an irregular, finger shaped wetting front because the water avoids zones of the soil that are, for any reason, less permeable than the rest of the soil. It happens frequently (Flury et al., 1994) and it is possible to divide it in three sub-groups (Owaga et al., 1999; Hendricks et al., 2001): macropore flow, funnel flow and finger flow (or unstable flow). Macropore flow is the movement of water through earthworm burrows, root channels, fissures and cracks, funnel flow is caused by textural boundaries, and refers to the fact that water can move laterally when it encounters a change in texture in the soil profile, and finger flow (or fingering) is the result of wetting front instability mostly due to air entrapment, water repellency and textural layering.

1.1.4 Macropore flow and funnel flow

Beven and Germann (1982) did a review on macropore flow. With the term macropore they implied "every structure that permits non equilibrium channeling flow, whatever its size". They argued that water flowing through macropores may have a much higher velocity compared to the water flowing through the soil matrix. This possibility increases with the size and connectivity of the macropores. Macropores, even though they constitutes a small part of the total soil volume, can be responsible for the major part of vertical flow in the soil. Beven and Germann (1982) divided macropore flow into three different stages. (a) The first stage occurs when precipitation is lower than infiltration capacity, in this case all the water is absorbed by matrix pores; (b) the second stage developes when the infiltration capacity is lower than the precipitation, that, in turn is lower than the flow through the macropores and infiltation capacity combined. In this case both matrix pores and macropores contribute to water flow. There will be lateral losses of water from the macropores to the soil matrix. (c) The third stage occurs when the precipitation is bigger than the infiltration capacity and flow through macropores combined, in this case things would be similar to the second stage with the difference that water will start ponding on the soil surface.

Jarvis (2007) also did a review on macropore flow. He defined macropore flow as "a non-equilibrium process whereby water at pressure close to the atmospheric one, rapidly

by-passes a drier soil matrix". That means that a wetting front loses its homogeneity as water starts to flow through conducting macropores rather than through the soil matrix. In order to have water flowing through the macropores the water pressure at the pore-matrix interface needs to be higher than the water-entry pressure. This leads to the fact that the higher the irrigation rate is, the easier it is for macropore flow to occur. It is also important to take into consideration the fact that the intensity of macropore flow is not necessarily proportional to the macroporosity. In fact, if the macroporosity is small, a larger portion of the macropores has to be water-filled in order to conduct the water at the set flow rate, meaning that more macropores will be hydraulically active (Larsbo, Koestel and Jarvis). Other factors that influence the occurrence of macropore flow are the duration of the irrigation, the initial soil water content and the hydraulic conductivity of the matrix. Taking into consideration that the pore size is not the only factor controlling macropore flow, it was suggested that pores with a diameter larger than 0.3-0.5 mm can be considered to be macropores.

An example of funnel flow (or heterogeneous flow) can be made: in a sandy soil a clay lens with a hole, or two clay lenses close to each other will redirect the flow in the hole or in between the two lenses creating, just, funnel flow. At low water content levels macropores have the same effect as clay lenses.

1.1.5 Finger flow

During the recent decades many studies on wetting front instability in layered soils have been conducted. The main outcomes are: (a) soil stratification enhances the formation of fingers, in fact the movement of the water through different layers creates a wetting front instability but just if the water moves from a fine texture layer to a coarse texture layer, in other words, if the irrigation rate is large enough, wetting front instability occurs if the top soil has a lower conductivity than the subsoil. The thinner the layers are the more fingers will be created (Glass et al., 1984; Hill et al., 1972; Sililo et al., 2000; Wang et al., 2018); (b) if the layers are discontinuous they creates both finger and funnel flow (Sililo et al., 2000); (c) water repellency differences between the layers contributes to finger flow formation and increases the maximum pathway depth of the water (Rye et al., 2017; Wang et al., 2018); (d) a single finger consists of a saturated inner core surrounded by an unsaturated layer (Hill et al., 1972; Liu et al., 1994; Rezanezhad et al., 2006); (e)

the width of the finger depends on the initial soil moisture, the higher it is the wider the finger will be, on the shape of the defect (aggregate, fractures etc.) of the soil that creates the finger and on the porosity, the larger it is the thinner the fingers will be (Cremer et al., 2017; Hill et al., 1972). In contrast with other studies Glass et al. (1984) found that the finger width depends even on the total flux. (f) Once the preferential flow is established it does not change over time (Glass et al., 1984); (g) surface depressions ease the formation of fingers; (h) If a finger impinges centrally an inclusion which is denser than the soil matrix its vertical propagation almost entirely stops while filling the inclusion, to be then reinitialized below the inclusion at the same location. The velocity of the fingers that impinges laterally on an inclusion remaines almost unchaged, the fingers continue to propagate vertically while just a small part of the water flows laterally in the inclusion (Cremer et al., 2017; Rezanezhad et al., 2006);

Even though when talking about infiltration it is common to think just about the vertical movement of water, lateral movement of water also plays an important role in the infiltration process. Ritsema et al. (1995) suggested the presence of a "distribution layer" at the top of the profile where the lateral movement of water is larger than the vertical movement. Water repellency facilitates the distribution flow (lateral movement in the distribution layer).

1.1.6 Water repellent soils

Water repellent soils are, as stated by the name, soils that repel water. They are not isolated cases. They are found throughout the whole world and in many different environments such as forests, brushlands, grasslands, agricultural lands and golf greens (DeBano, 1981). Water repellency is a characteristic with a big influence on water flow through soil as it prevents normal infiltration of water making soils resist wetting for periods that could last weeks. It is caused when hydrophobic films, usually formed by plants waxes, microbial activity or other organic material, form around the soil particles. In addition to this, water repellency can be induced by heat. Many studies (DeBano, 2000; MacDonald et al., 2004; Hubbert et al., 2006) state that wildfires are a major cause of water repellency in soil. Water repellency has many consequences, it facilitates non-uniform flow, so water flows through prefered pathways leaving big volumes of soil dry. It reduces infiltration capacity, it facilitates overland flow and soil erosion, it influences

evaporation and the water balance of soil (Leelamanie et al., 2008; Doerr et al., 2000). Theoretically the wettability of a soil should increase over time when in contact with water (DeBano, 1981), that means that the more a soil is in contact with water and the less water repellent it is. There are many ways to determine whether a soil is water repellent or not: WDPT (water drop penetration time), equilibrium liquid-solid contact angles and energetics of the soil-water-air interface (DeBano, 1981). WDPT is a test that consists in measuring the time until complete penetration of a drop of water placed on the soil surface (Leelamanie et al., 2008; Bughici et al., 2016). According to Wang et al. (2000) in water repellent soils water starts to infiltrate when the ponding time exeeds the WDPT. WDPT determines how long water repellency persists on a porous surface (Doerr et al., 2000). It is difficult to state whether a soil has a high or low degree of water repellency because the perception about it varies extensively, the same value of water repellency can be consider high or low depending on the situation.

1.1.7 Antecedent soil moisture

Many studies on the effect of antecedent soil moisture on water flow through the soil were made. The conclusions were that: (a) antecedent soil moisture does not affect the percolated volume of water through the soil (Granovsky et al., 1994; Shipitalo et al., 1996); (b) the higher the antecedent soil moisture level is the bigger is the portion of soil that contributes to water flow, resulting in a smaller chance to create preferential flow (Granovsky et al., 1994; Shipitalo et al., 1996); (c) during an irrigation, if preferential flow does not occur, most of the percolated water of a wet soil sample is water displaced from the soil matrix and not the irrigation water (Shipitalo et al., 1996); (d) initial soil moisture content stabilizes the wetting front if it is homogeneously distributed, otherwise, if it is heterogeneously distributed it eases preferential flow as water prefers to flow through the already wetted zones (Glass et al., 1984); (e) Initial water content influences the finger width, the higher it is the wider the finger will be (Liu et al., 1994); (f) soil water content influences water flow velocity through soil but researchers seem not to agree on whether it increases or decreases it. In fact, Jaynes et al. (2001) found that the higher initial water content is the faster the water will flow through the soil, while the experiments carried by Hardie et al. (2011) resulted in a deep and fast water infiltration in low antecedent soil moisture conditions and in a much smaller depth and water infiltration velocity in high

initial soil moisture conditions. This, at odds with the other studies as it, means that high initial water content slows down water infiltration through the soil.

1.2 X-ray imaging

X-rays have a wavelenghth ranging from 0.03 nm to 3 nm and a frequency between 30 PHz and 300 EHz. They can be used for imaging the inside of objects since they have the ability to go through thick objects, of certain materials, without being reflected or scattered. Even though, hystorically, x-ray imaging has been mainly used for medical purposes, since the 1980s it has been gaining succesful applications in other fields such as environmental and soil science, biology, and geo-chemistry for three main reasons: (a) X-rays scanners became more affordable, (b) the image processing software has developed sufficiently that no programming skills are required to analyze the images and (c) computers have become powerful enough to elaborate the large amount of data generated with X-ray imaging. The probably most important characteristic of x-ray imaging is the fact that it is a non-invasive technique, and this facilitates the monitoring of an experiment in opaque materials like soils without compromising it.

Not many studies were done using X-ray computed tomography, in fact I am not aware of 2D approach infiltration experiments conducted using X-rays. The main advantage this technique offers is the possibility of doing a non-destructive analysis of the sample (Cnudde et al., 2013). A practical example can be made: to examine water flow patterns with an X-ray machine allows you to see the exact water pattern while if it is done in the field with a tracer to be able to see the water flow pattern an excavation is needed and that spreads a bit the tracer on the soil profile modifing the water flow pattern. X-ray imaging is often used for 3D imaging of samples as it offers, in combination with dedicated software pakages, the possibility to quantitatively and visually analyse the structural characteristics of the sample such as pore size distribution, fractures, macropores etc. An important downside of this thechnique is that it is diffucult to do a reliable comparison between experiments unless the X-ray machine was set up identically and the image analysis procedure done in the same way. That is because there is not a standardized method for X-ray imaging, since all the machine parameters can be choosen by the operator. The same is true for the image analysis. In fact Baveye et al. (2010) showed how the thresholding of an image can lead to different results depending on the operator.

1.3 Aim

The goal of this thesis is to understand how soil water repellency and structural pores influence waterflow through soil, with special attention to preferential flow. This study aims to understand what is the role of plants in water repellency and how they influence water flow. This project focuses on soil with identical texture but different structural pores network and water repellency. Furthermore, it aims to see how infiltration patterns vary over time during the same irrigation of the samples and if they remain the same if the samples are subjected to many irrigations letting the soil dry after every one of them. It also aims to verify whether x-ray computed tomography is a valuable option for this kind of researches.

2 Material and methods

2.1 Experimental set up

The experiment configuration was as follows: two-dimensional experiments were carried out to monitor the infiltration of water through different types of repacked soil samples (bare soil, sown soil and garden soil samples). To do so, quasi 2D boxes (they recreate a 2D environment) for the soil samples and an irrigation device that fits the pump used for the experiment were designed. The infiltration experiments were performed inside an X-ray scanner.

2.2 Box design

Instead of using a ready made box, it was decided to design it using the Autodesk program Fusion 360 and to print it with a 3D printer because specific characteristic were needed (the printing was done by Daniel Isekog). The 3D printer used was the "Ultimaker 3 extended" and the printing material is X-PLA from AddNorth. X-PLA is a 100% biodegradable thermoplastic with a high impact resistance. As shown in Figure2 the complete design was made of two boxes, a frame, two easels and a top part. The first box contained the soil under examination and its dimentions are 15 x 15 x 1 cm, it was designed with such a small thickness for two main reasons: (a) the x-ray machine used for this experiment cannot get any information in the direction of the X-ray beam when doing 2D images and (b) the thicker the object to scan is the more energy for the X-rays to go through it is required. The problem with using high energy is that the image will exhibit lower contrasts because more of the X-rays travel through the object without interaction. The walls of the box were designed uneven to reduce preferential water flow along them. Another, smaller box (15 x 7.5 x 1 cm) was used for drainage. It is filled with sand so that the water could flow from the first box to the second without creating a seepage face. The drainage box was separated from the first by a permeable cloth. At the bottom of the drainage box was a grid that allowed the water to flow out of it in a tray used to collect the water. Furthermore, a frame, two easels and a top part were designed. The frame was used to connect the two boxes. The easels were used to stabilize the boxes and to avoid the lower one to touch the floor letting the water flow out of it. The roof-like top

part was of fundamental importance because, without it, the water drops falling on top of the walls were likely to flow in the box causing a greater irrigation at the sides. With it the water drops falling on the top of walls were forced to flow outside the box.

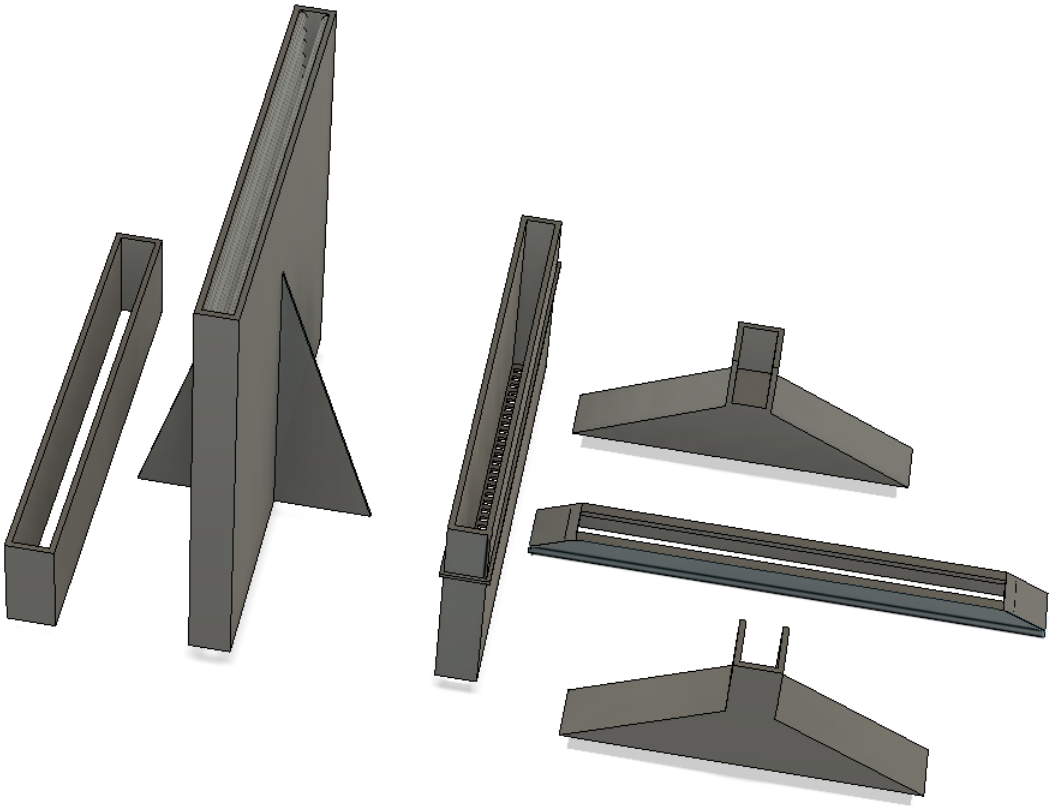

Figure 2: From the left: frame, main body (the two supports attached to it were needed for the printing, after it they were removed), drainage body, two easels and the top part

2.3 Irrigation device

The design of the irrigation device (done by Daniel Iseskog) was based on the box dimensions. It was controlled using an Arduino microcontroller kit. As shown in Figure3 the irrigation device was composed by a main body, where the Arduino board and a moving body were attached, and a pump. The pump had two hoses. The first was for the supply of water from a tank, and the second was attached to the moving body and ended with a needle, for the irrigation. The functioning of it was made with in a very simple way: it kept moving from one side of the box to the other, velocity of the moving body and irrigation rate of the pump were regulated respectively using the arduino and the pump display. To prevent the overheating of the engine driving the device, the needle was

stopped for a second at each side. As a result of that, to avoid a greater irrigation on the sides of the box, the needle movement was larger than the box width so that the needle was dripping outside of it during the stops.

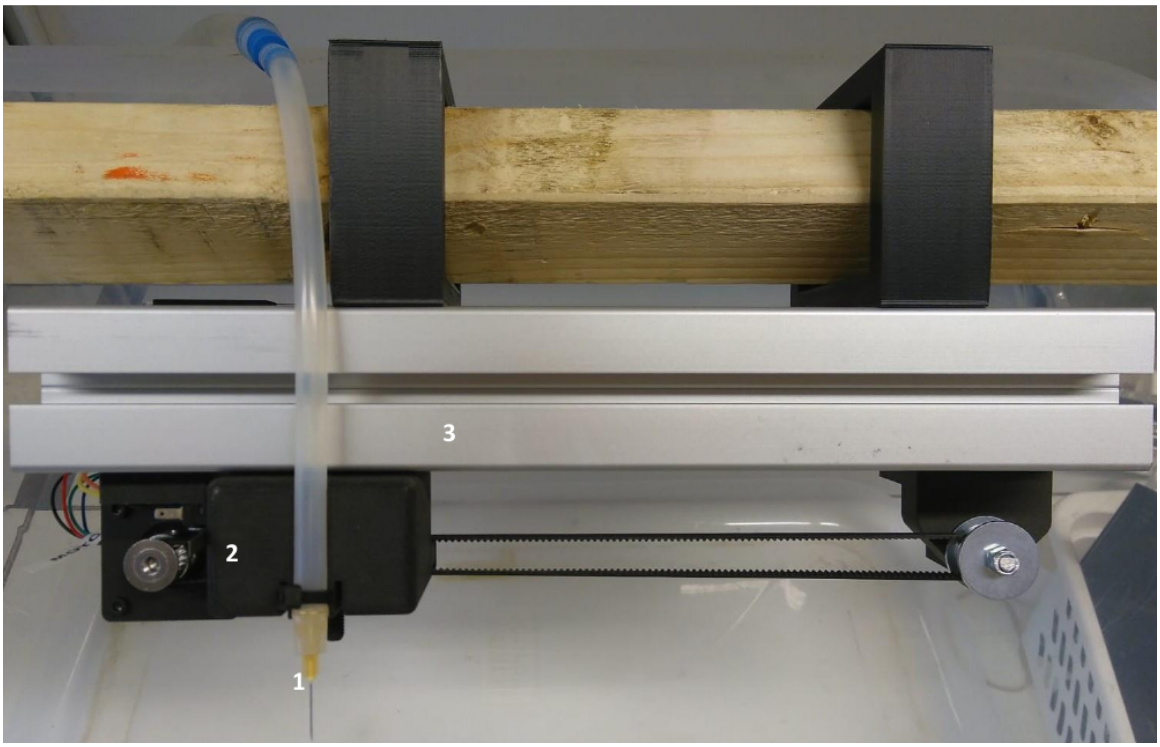

Figure 3: Irrigation device. Needle (1), moving body (2), main body (3)

2.4 Implementation of the set up

In order to do this experiment a few adaptions to the x-ray machine were needed. The first thing that needed to be changed was the rotating platform used to place the samples. The rotating motion is needed for 3D images but for 2D images the sample has to be motionless. Because of that it was decided to replace it with a stool adjustable in height. The platform was not removed from the machine but just moved so that there was enough space for the stool to fit in the x-ray machine. The second adaption was to find the place where to attach the irrigation device inside the x-ray machine (Figure4). It was attached to two threaded vertical poles that are part of a moving frame installed on the ceiling of the x-ray machine for a previous project. Then, the pump and a water tank were placed in the x-ray machine inside a plastic box so any eventual leakage would go in the box without damaging the machine. All the hoses and electric cables were tied up to the walls so that they were not in between the x-ray source and the detector. To remove all the

air from the hose it was necessary to place it so that it was always going upwords. In the last part, where it was connected with the needle, a T-shaped connector was built in so that it was possible to remove the air even in that bended part.

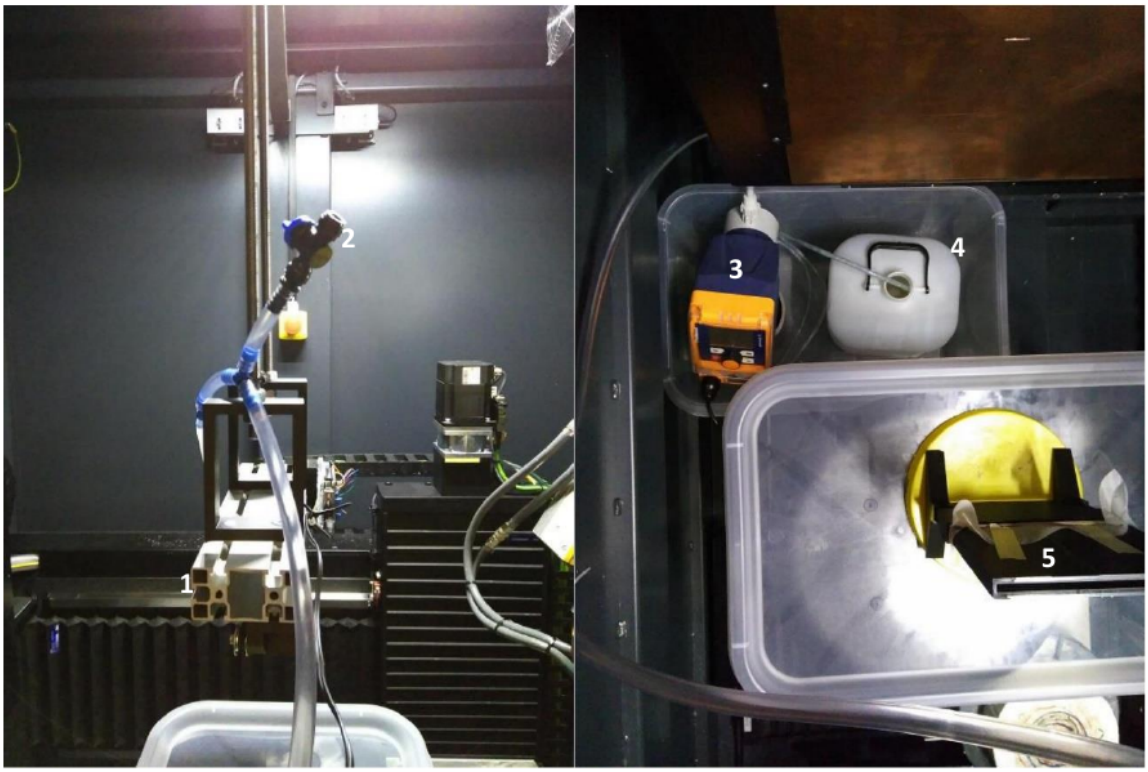

Figure 4: at the left: irrigation device (1) (seen from the side) set in the x-ray machine, T-shaped connector (2). At the right: pump (3,) water tank (4) and soil sample (5) seen from above

2.5 Set up testing and optimization

To get to the final experimental set up many test irrigation runs were carried out. At first the test irrigations were made in the laboratory, with the goal of testing the irrigation device to be sure that the pump met the requirements needed for the experiment. During the laboratory tests the speed, the distance covered by the needle movement, the stopping time of the needle at each end of the movement and the irrigation rate were determined. To recreate a realistic scenario the optimal flow rate to apply to the soil samples would be the average rainfall intensity observed in the field where the samples were taken, which is roughly 1 mm per hour. The pump, however, was not able to have an homogeneus irrigation at such small rates (while connected to the needle) so it was necessary to use a

much higher value, 53.33 mm/hour (80 mL/hour). More irrigation tests inside the x-ray machine were carried out in order to analyse the resulting images so that it was possible to see if the set up needed improvements. It was during these tests that it was decided to make the needle cover a distance larger than the box width. This adjustment was done to avoid a greater irrigation rate at the edges of the box caused by the one second stop of the needle. In this way, the water was dripping outside the box during the stops. This expedient was not enough to avoid a greater irrigation rate at the edges of the box because some of the drops that hit the top part of the side walls managed to flow inside the box, so it was necessary to design an extra part to put on top of the box (the "top part" mentioned above).

2.6 Sample preparation

Water drop penetration time (WDPT) tests were conducted on both soil and peat materials. The soil used for the experiments is a sandy loam soil (Koestel et al., 2019). The soil did not show any sign of water repellency as the water drops infiltrated into the soil in less than a second, but peat, if completely dry, resulted strongly water repellent as WDPT was 30 seconds. Five replicas of each sample type were prepared. Ten boxes were filled with a mixture (50-50) of soil and peat. In five of them different species of plants were planted. The planted species are *Trifolium incarnatum*, *Trifolium repens*, *Lathyrus odoratus* and *Lupinus regalis*. Moreover, additional five boxes were filled with soil and only installed in a garden plot close to the SLU campus for four weeks so that the natural vegetation, micro and macrofauna could create structure in the samples. In the following, the bare samples filled with the soil-peat mixture will be denoted as bare soil samples, those cropped plants will be referred to as sown soil samples and those that were incubated in the garden will be called garden soil samples. The preparation of the sown samples was as follows: a permeable cloth was attached to the bottom of the boxes so that it was possible to fill them with the soil-peat mixture, then they were immersed in water until 2/3 of their height to bring the soil close to water saturation. Once the soil was wet enough the boxes were removed from the water and the plants' seeds put in the boxes, covered with some wet soil and a perforated plastic foil to avoid evaporation. One week after the sowing, when the seeds had sprouted, the plastic foil was removed and a cultivation lamp was set installed to provide sufficient light for the plants to grow.

2.7 Irrigation experiments

The maximum flow rate appliccable to the soil samples without overflowing them is equal to their saturated hydraulic conductivity, which was estimated to be around 80 mm per hour. This estimation was based on measuring the discharge of water from a saturated sample under a steady irrigation rate. Once the soil was saturated the irrigation was increased untill ponding took place. This value is meant to be just an approximate upper limit value for the irrigation rate as K_s (saturated hydraulic conductivity) can vary depending on the soil structure and over time during the same infiltation and different values can be obtained if the experiment is repeated (Snehota et al., 2015). The main reasons why it varies over time are air entrapment (Faybishenko, 1995; Zlotnik et al., 2007) and changes in the surface characteristics during rainstorms or irrigations (Fohrer et al., 1999).

Subsequently, the irrigation device was set up in order to avoid the irrigation drops to hit always the same spots of the soil surface and to be sure that the irrigation would cover the whole width of the box. The boxes were irrigated with a flow intensity of 80 mL/h (53.33 mm/hour). The sown soil samples were irrigated even with an additional irrigation rate equal to 160 mL/h (106.66 mm/hour). Every irrigation was reapeted five times and between each experiment the samples were let to dry in a drying room for 20-22 hours at a temperature of 35.5 °C, this time was not enough to dry the sample completely.

2.8 X-ray imaging

Once the sample was in place, the last thing to do before starting the scan was adjusting some parameters values in order to improve the quality of the images. These parameters are: (a) power: the higher it is and the more x-rays pass through the sample, but the image will have less contrast so it is recommended to keep it al low as possible; (b) timing: it is the time used from the machine to get a single image, the higher it is and the brighter the image will be; (c) number of radiographs: it is the number of images per scan, it is directly proportional to the quality of 3D images; (d) average: it indicates the number of pictures taken from the same angle; (e) skip: it tells how many picture the machine considers (e.g. if skip is equal to 2 the machine considers every second picture); (f) binning: it combines the detector crystals so it is possible to improve or reduce the

resolution; (g) sensitivity: it determines how sensitive to the x-ray the detector is; (h) amount and thickness of copper filters: they are placed in front of the x-rays source to remove the low energy parts of the x-ray spectrum. The values used for both 2D and 3D scans are shown in Table2.

Table 2: X-ray machine settings

X-ray machine set up		
	2D images	3D images
Image size	997 x 1012	2024 x 2024
Power (voltage)	500 μA	500 μA
Power (current)	120 kV	120 kV
Timing	131 ms	131 ms
No. of radiographs	7000	2000
Average	1	2
Skip	0	1
Binning	1 x 1	2 x 2
Sensitivity	1.00	2.00
Thickness of copper filters	1.2 mm	1.2 mm

For every experiment a first scan of 50 images without irrigation was done to obtain the image of the dry sample which was needed later for the image analysis. After that, a scan of 7000 images was done while the irrigation device was working. For the experiments where the water flowed slower than usual it was necessary to run an extra scan. All the images were directly saved into a computer connected to the x-ray machine.

2.9 Images of the 3D soil structure

The set up used to obtain the 3D images was not the one described previously but the standard one of the X-ray machine. The 3D images were obtained before and after the irrigation experiments so that it was possible to compare them. An average of the 2D

images composing each 3D image was done in order to obtain the density of the samples. In Figure5 it is possible to see an example of an image at every step of the process. In the two images, the gray value is proportional to the average density in the direction of the X-ray beam, the brighter it is the denser the sample is.

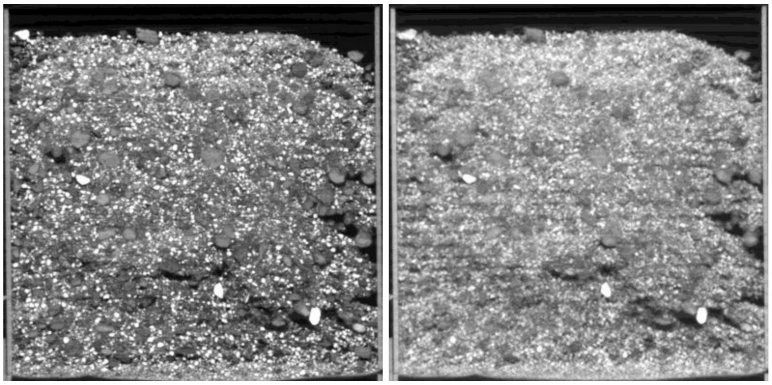

Figure 5: From the left: one slice of the 3D image, average image of all the slices of the 3D image, (bare soil sample 3)

2.10 Wetting front images

The software used to analyse the images was ImageJ. The analysis of the wetting front images can be divided into three steps: (a) image preparation, (b) image segmentation and (c) image analysis.

2.10.1 Image preparation

The images preparation was done as follows: the first step was it to create an average image of the 50 dry images, then to obtain the wetting front images from the row data the dry image was subtracted from the wet ones; all the images were put in sequence in order to create a movie of the wetting front. To reduce the huge amount of data (on average during an experiment consisted in 7000 images) a 5 seconds step average was done (average of five consecutive images every five seconds, the images that were not used for the average were discarded). All these passages were automated with a plug in. Then, the movies were reduced in size by a factor of 0.25 because it is easier to work with small images. Next, a median filter with a radius of 3 pixels was applied to reduce the noise. After this step, the images were ready for the segmentation.

2.10.2 Image segmentation

Image segmentation is a technique used for dividing an image into differnt regions that are internally homogeneus according to specific characteristcs like the grey scale or texture (Lucchese et al., 2001). It is done to simplify the image and enable the analysis described in the following.

2.10.2.1 2D images

The segmentation of the 2D images was carried out on every 50^{th} image of every movie (one image every 4.17 minutes). The segmentation procedure for a single image was the following: The first thing to do was to convert the image into a binary image (black and white). The threshold algorithm used for this process was the default one of imageJ, a specific version of the IsoData algorithm (Ridler et al., 1978). Then, since the image regions shouldn't have any small holes inside (Lucchese et al., 2001), they were removed. At this moment the water was displayed as white and the rest as black. Then, the image was outlined to get an image were everything is black but the water perimeter. The easier way to continue was to use the 3D Objects Counter determining a minimum size (e.g. 150 square pixels) in order to remove all the objects (isolated water drops) smaller than the decided limit obtaining an image with just the wetting front, but this method worked out just for half of the images so the selection was made manually. Figure6 shows an example of an image at every step of the segmentation.

2.10.2.2 3D images

The segmentation of the 3D images was done to quantify the pore distribution in the samples. After the segmentation was done, an average of all the images composing the 3D segmented image was done in order to capture the macroporosity of the samples in a 2D image. For visualization purposes the threshold algorithm used for the segmentation was the same used for the 2D images in order to have the possibility to compare them. Figure7 shows an example of the final result.

2.10.3 Image analysis

The first analysis to be made was a visual comparison between the flow patterns to verify whether they changed or remained the same during consecutive irrigation runs. This was

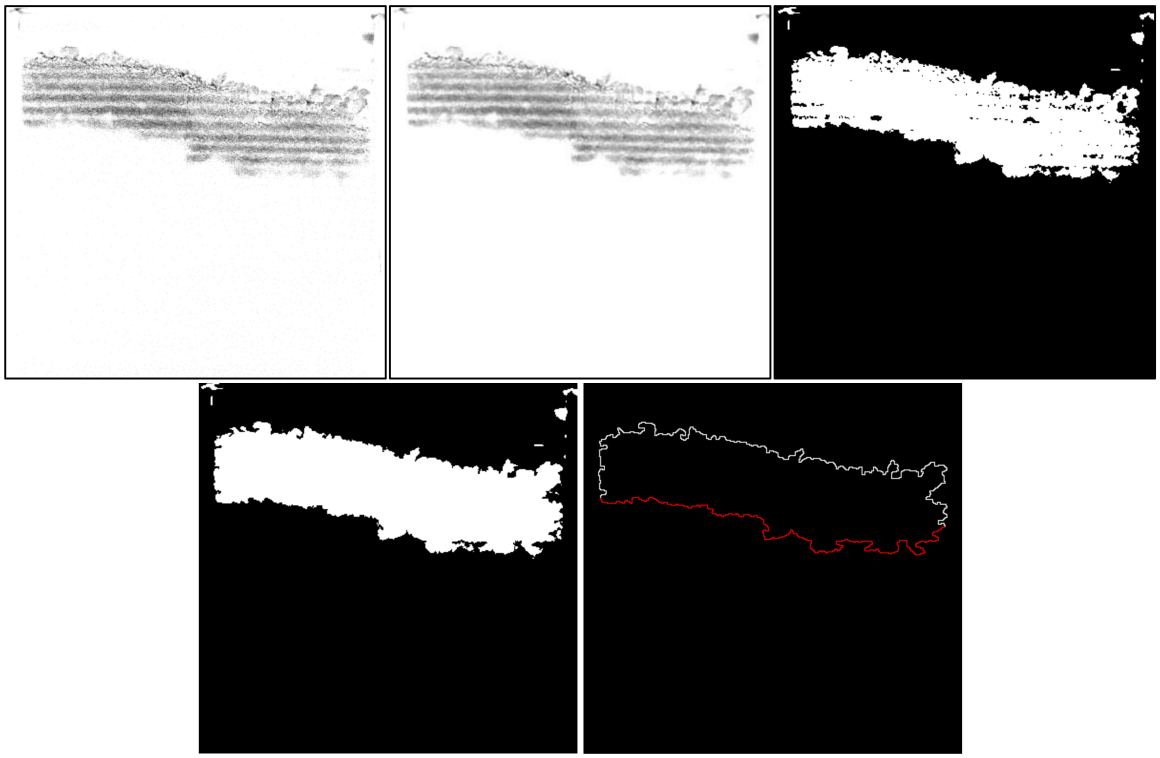

Figure 6: First row from the left: original image, image after application of median filter, image after conversion to binary. Second row from the left: Image after "Fill Holes", image after "Outline", in red the wetting front (bare soil sample 1)

done by overlaying the flow patterns of one sample obtained during the different irrigation runs.

A visual analysis was made even to evaluate whether the plants created water repellency in the soil.

To analyse the wetting front, a tortuosity index was calculated. This index is equal to the width of the box (in pixels) divided by the number of pixels that make-up the wetting front. Both the width of the box and the number of pixels composing the wetting front were calculated using ImageJ, the width was calculated on an image where the walls of the box were clearly visible while the number of pixels composing the wetting front manually selecting the wetting front on the segmented image. These measures were done every 50^{th} image of every movie so that it was possible to see the trend of the tortuosity index. The index values are always between 0 and 1, the smaller it is the more tortuous the wetting front is. Smaller tortuosity indices indicate preferential flow. This is because preferential flow increases the area of contact between the wetting front and the soil, so the number of pixels composing it in the image increases while the box width remain the same.

Another parameter that was calculated was the mean velocity of the infiltration and it was done using the following formula (1):

$$V = \frac{Y_w - (Y_s + c)}{t} \tag{1}$$

Where V is velocity(cm/min), Y_w is the average distance of the wetting front from the top of the image (mm), Y_s is the average distance of the soil surface from the top of the image (mm), c is a correction factor (mm) to adjust the soil surface position for the samples with plants. In these images the soil surface position was masked by the water that was withheld between the plants' stems. The correction factor was set to 0 mm for bare soil samples and garden soil samples and to 5 mm for sown samples. t is the time (min).
The last analysis made was the comparison between the 3D images done before the irrigations with the ones done after the irrigations to see if there were any changes in the structure of the samples.

3 Results and discussion

3.1 Soil structure and macroporosity

In Figure7 it is possible to see an example of the macroporosity of the samples, the gray value is proportional to the average density in the direction of the X-ray beam.

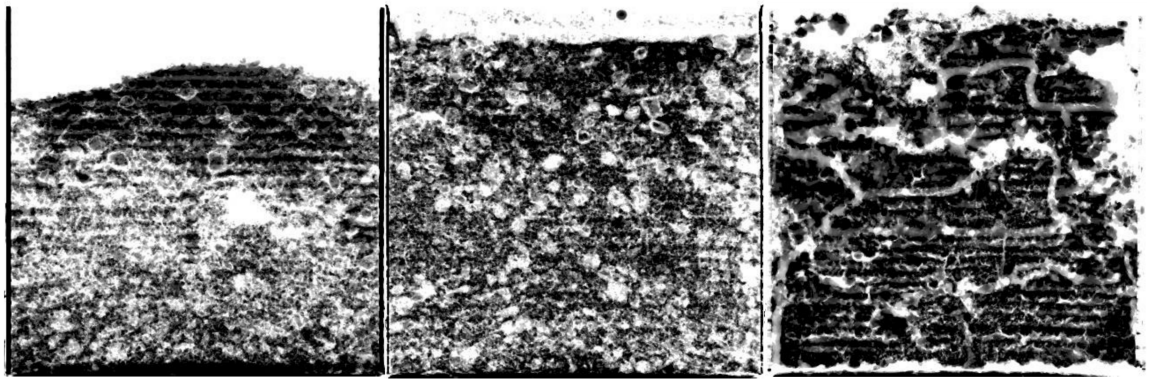

Figure 7: Macroporosity of (from the left): bare soil sample 3, sown soil sample 1, garden soil sample 4

It is evident that the matrix of the garden soil samples was denser than the other samples, this is because it was composed just by soil while the other samples were made with both soil and peat. The bare soil samples and the sown soil samples were more densely packed in the top part. The garden samples contained the biggest macropores.

3.2 Wetting fronts comparison

The visual comparison of the wetting fronts yielded completely different results between the experiments regarding bare, sown and garden samples. As shown in Figure8 the bare soil samples usually produced a fingered wetting front and the infiltration pattern tended to remain the same (just small differences can be noted) when the experiment was repeated with the same irrigation rate. The only infiltration pattern differing from the others was the one of the first irrigation run (the red color in Figure8) that was done when the sample was completely dry. In fact, the initial water content highly influenced water flow through soil: decreasing it increases the infiltration rate but, at the same time, decreases the velocity at which the wetting fron moves (Gray et al., 1967). The first irrigation's wetting front pattern is different from the others in the images because the

wetting fronts were compared at a certain time and not when they reached the same depth. This was done so that it was possible to compare the images with the wetting front tortuosity graphs. Comparing them when they reached the same depth would show, most of the times, a good match beetween all the wetting front patterns.

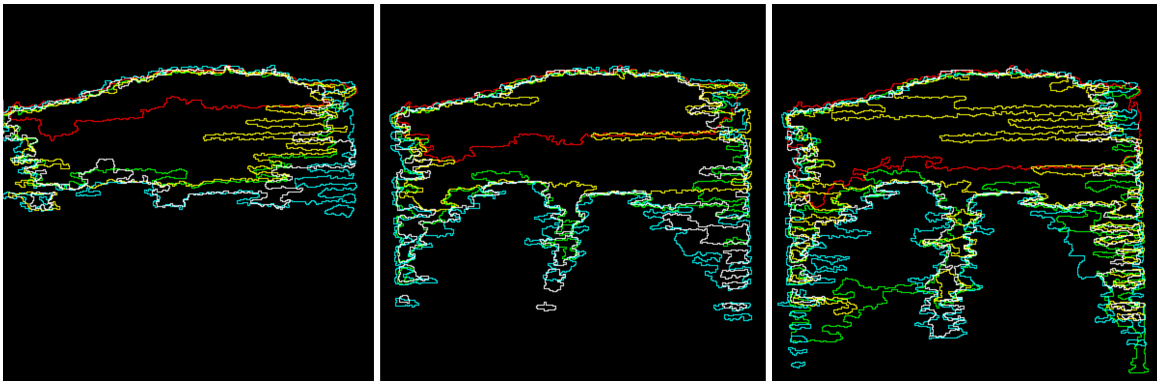

Figure 8: Wetting fronts of all the irrigations done to bare soil sample 3 after (from the left): 4.17, 8.33 and 12.50 minutes. Red=first irrigation, green=second irrigation, yellow=third irrigation, white=fourth irrigation, blue=fifth irrigation

A different situation was encountered analysing the images of the sown samples (irrigation rate of 80 mL/h) (Figure9): (a) the wetting fronts tended to be more homogeneus than the ones in the bare soil samples and (b) there was not the repetition of the same infiltration pattern during different irrigations if compared at a certain time. Raising the irrigation rate to 160 mL/h made the infiltration patterns more similar to each other but they were still considerably different in between different repetitions.

In Figure9 it is possible to notice, in the left image of the second row, an error of the segmentation process. The yellow wetting front is very high up in the sample even if in reality it was not. The segmentation results were not always perfect and it happend that one image every once in a while was not well segmented.

The wetting fronts of the garden samples tended to have a trend similar to the one of the bare soil samples. Apart from garden sample 2, the patterns of the different irrigation runs were similar to each other, an example is shown in Figure10. Preferential flow was present even in these samples but fingers tended to be lower in number and wider in x-direction compared to the ones in the bare soil samples. In fact, while in the bare soil samples there usually were two or three fingers, in the garden samples it was more common to notice just one big finger. This is largely credited to the difference in structure between the two

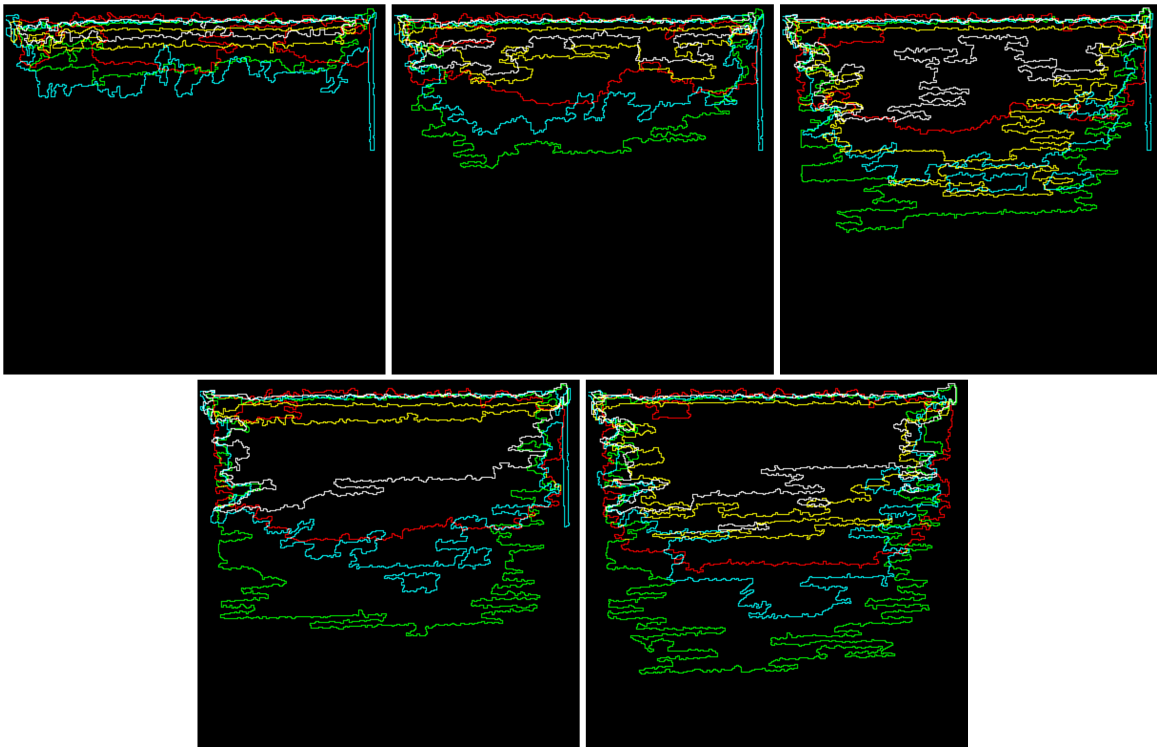

Figure 9: Wetting fronts of all the irrigations done to sown soil (80 mL/h) sample 2 after (from the left): 4.17, 8.33, 12.50, 16.67 and 20.83 minutes. Red=first irrigation, green=second irrigation, yellow=third irrigation, white=fourth irrigation, blue=fifth irrigation

sets of samples, in fact the number and size of the macropores in the garden samples were significantly higher than the ones in the bare soil samples.

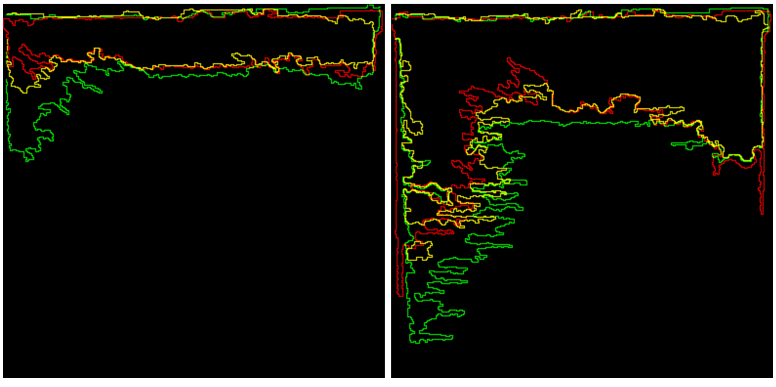

Figure 10: Wetting fronts of all the irrigations done to garden soil sample 3 after (from the left): 4.17 and 8.33 minutes. Red=first irrigation, green=second irrigation, yellow=third irrigation

Comparing the wetting front patterns with the 3D segmented images, it is possible to

notice a relation between the flow pattern and the macroporosity of the samples. Taking as an example the bare soil sample 3 (Figure7 and Figure8: left side) it is possible to notice that the water flowed through the denser parts of the sample. This happend probably because the water pressure at the macropores-matrix interface was not enough to establish macropore flow, so the water flowed through the matrix avoiding the macropores.

3.3 Average infiltration velocity

Looking at Table3 we can clearly see that plants strongly influenced the infiltration velocity of water in fact, the average infiltration velocity in the sown samples irrigated with a rate of 80 mL/h was clearly lower than the one of the bare soil samples.

Table 3: Mean of the average infiltration velocities of each sample

Average velocities (mm/min)				
	Bare soil	Sown soil		Garden soil
Irrigation rate (mm/h)	53.33	53.33	106.66	53.33
Sample 1	7.46	2.95	7.40	5.74
Sample 2	5.53	3.32	7.17	5.95
Sample 3	5.02	2.47	7.12	7.52
Sample 4	6.08	5.56	8.92	7.11
Sample 5	5.68	5.62	7.92	8.28
Average	5.95	3.98	7.71	6.92

This big difference is due to the fact that in 3 sown samples, irrigated with a rate of 80 mL/hour, there were cases of possible water repellency. In more detail, it happend two times in sample 1, one time in sample 2 and one time in sample 3. When it happend in sample 3 and the second time in sample 1 the water didn't even start to infiltrate through the soil (after 12.50 minutes, time taken into consideration for the calculation of the velocity) while in the other two occasions the water managed to infiltrate just through small sections of the surface (Figure11). It is difficult to confirm that it actually was water repellency because, if water repellency occurred in a sample, it was expected

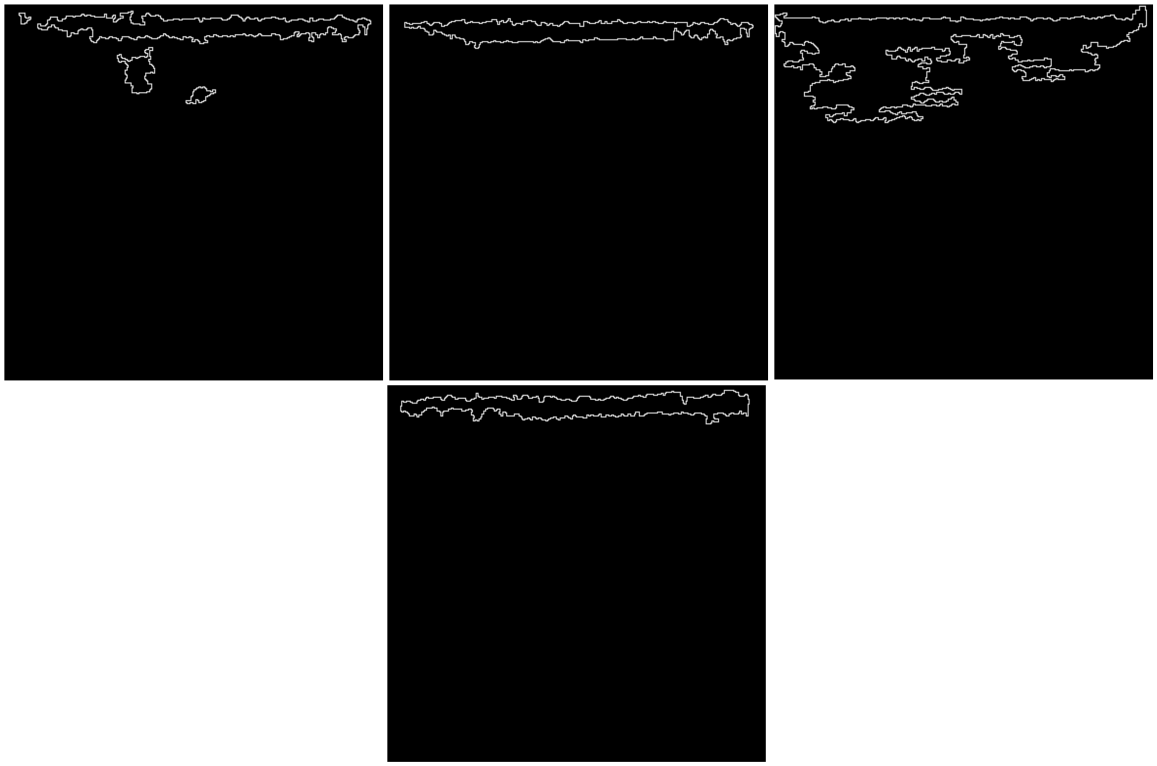

Figure 11: first row from the left: sown sample 1 third experiment, sown sample 1 fifth experiment, sown sample 2 fourth experiment. Second row: sown sample 3 third experiment. Every image represents the situation of the wetting front after 12.50 minutes

to see it fade throughout the different experiments or, if it was strong enough, not to see it fade at all. In this case water repellency happend during the third and fifth experiment of sample 1, during the forth experiment of sample 2 and during the third experiment of sample 3. The question is "how is it possible that a soil that didn't show any sign of water repellency and that is under conditions that should decrease it (multiple irrigations) suddenly shows them?". During the attempt to get heat induced water repellency in soil it was noted that if peat is completely dry it shows strong signs of water repellency, since after every irrigation the samples where let to dry in a drying room it could be that the samples surface got dry enough to get the peat to be water repellent. If that assumption is correct, and so the cause of the water repellency events was the peat. It also means that the plants had nothing to do with it or just gave a minor contribution and affected the infiltration patterns just by creating structure.

Another thing that can be understood well from Table3 is the huge effect that macropores have on the water infiltration velocity in the soil. In fact the more macropores there are in a soil, the bigger the permeabilty will be and the higher the water infiltration velocity

will be. The average velocity of water in the garden soil samples is the 15% higher than the one of the bare soil samples with the same irrigation rate. This percentage increases up to 23.2% excluding the bare soil sample 1 values that are completely different from the values of the other bare soil samples.
The infiltration velocity after 12.50 minutes of the first experiment of each sample was always smaller than the one of the other experiments for the bare soil samples. For the sown soil samples irrigated with a rate of 80 mL/h it was like that two times while for the sown soil samples irrigated with a rate of 160 mL/h and garden samples it was like that four times. Regarding the sown soil samples irrigated with a rate of 160 mL/h it was like that probably because, thanks to the high irrigation rate, it took just a little time for the samples to reach the initial water content of the other experiments. The fact that, during the first irrigation, the samples reached the initial water content of the other experiments in a short amount of time allowed the water to move roughly at the same velocity in every experiment.

3.4 Water repellency

Unfortunately we did not detect any water repellency on the sown soil samples, maybe because of the very short growing time (one month). There were a few cases of possible water repellency but they were not to be attributed to the plants but to the dry peat aggregates inside the samples. These very few cases of water repellency are not enough to draw conclusions on its effects on water infiltration through soil.

3.5 Wetting front tortuosity

Also the wetting front tortuosity values showed differences between the different samples. Looking at Figure12 it is possible to see the trend of the wetting front tortuosity index in a bare soil sample and notice two main things: the values for the first irrigation are much higher than the other irrigations values and the trend of the tortuosity index of all the other irrigations are very akin to each other.
A similar situation can be described for the soil samples with plants irrigated with a rate of 160mL/h (Figure13): values for the first irrigation tend to be higher compared to the other irrigations values but in this case the trend of the tortuosity index of all the other irrigations are not always similar.

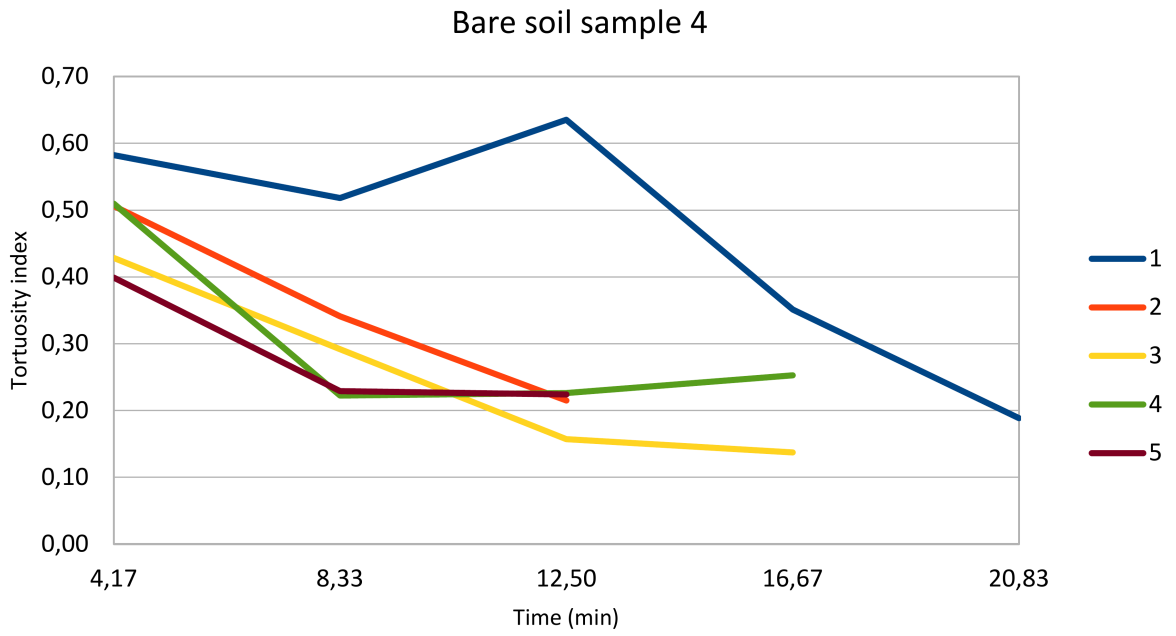

Figure 12: Bare soil sample 4 tortuosity index trends

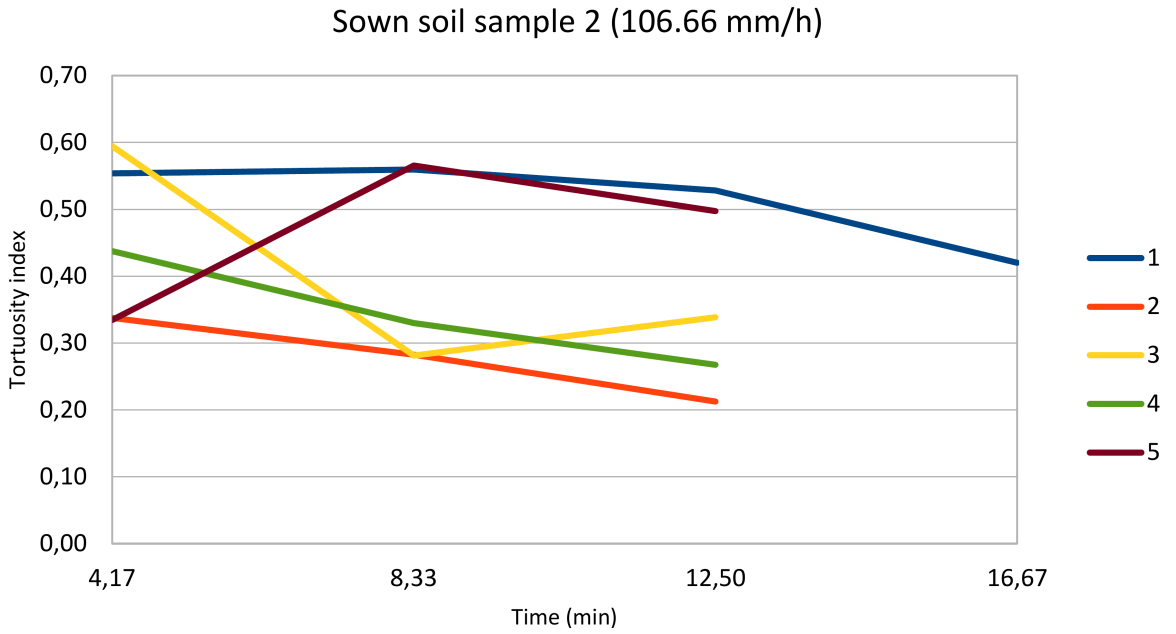

Figure 13: Sown soil sample 4 tortuosity index trends (irrigation of 160mL/h)

Regarding the ones with an irrigation of 80 mL/h (Figure14) there is not a clear trend between the different replicas. It happens to see the values of the first irrigations to be lower than the values of the other irrigations. There is not a clear trend between the values of the subsequent irrigations. The very high peak of the third irrigation is due to the error mentioned in the previos section. Analysing the third and fourth irrigations, however, we can assume that there would have been a peak anyway since the trends of

the two irrigations are very similar.

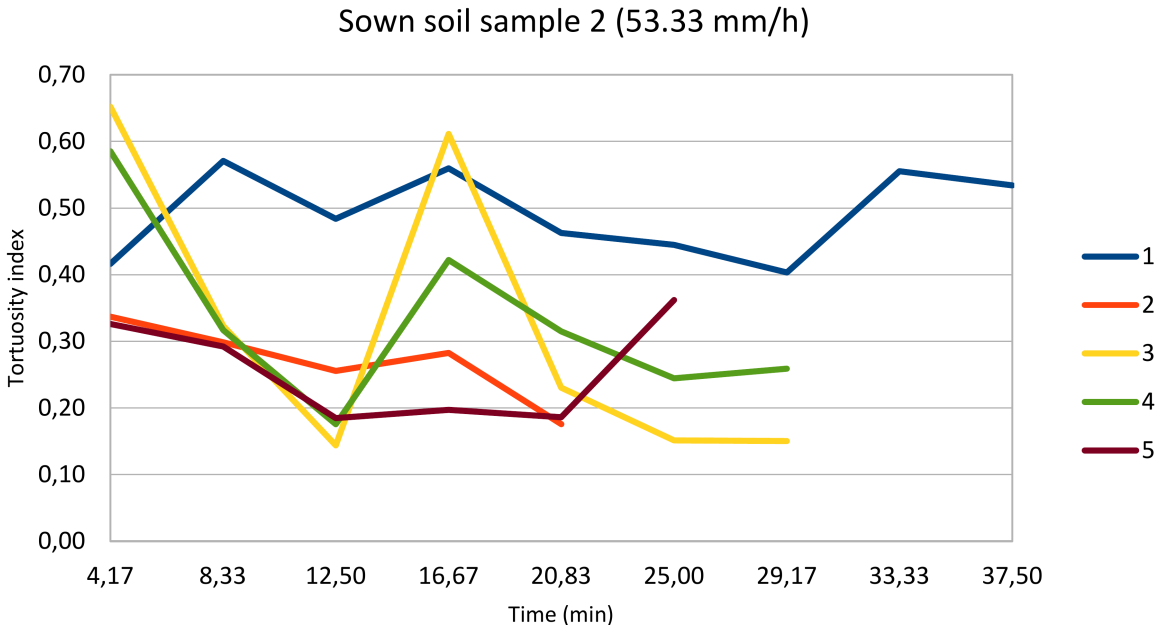

Figure 14: Sown soil sample 4 tortuosity index trends (irrigation of 80mL/h)

Talking about the garden samples the situation changes again. The values of the first irrigation are roughly the same of all the other irrigations. Excluding just a few exceptions all the tortuosity index trends are very akin to each other (Figure15) meaning that the initial water content did not effect the wetting front tortuousity.

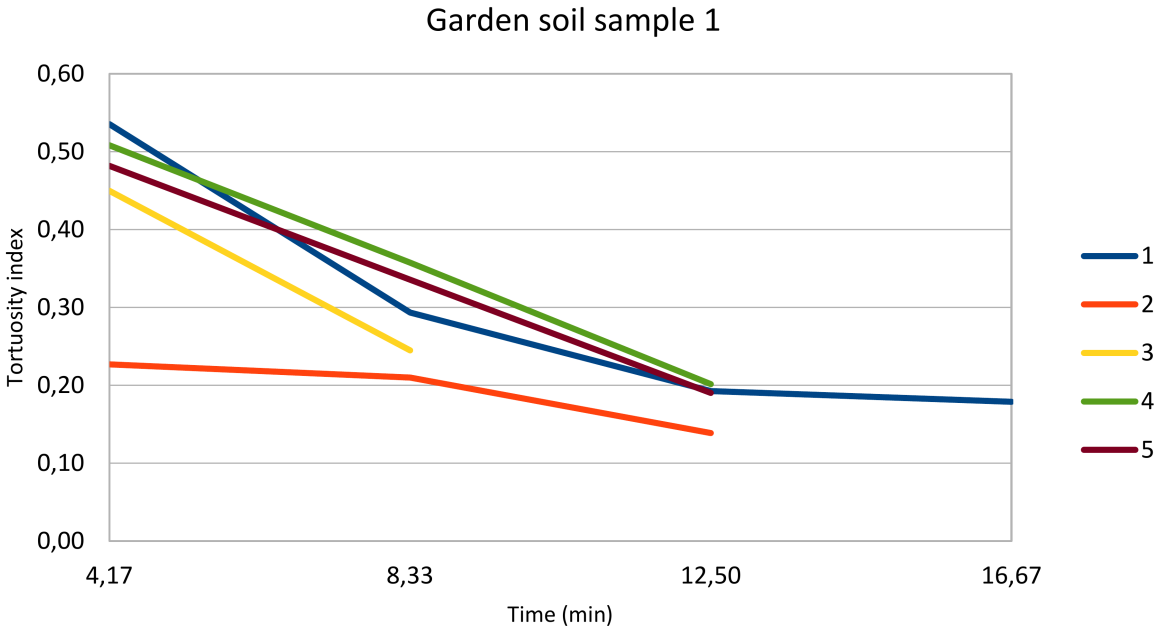

Figure 15: Garden soil sample 1 tortuosity index trends

3.6 Samples structure changes

There were different results even regarding the samples structure. As shown in Figure16 the structure of the bare soil samples significantly changed during the irrigations. In fact after the irrigation experiments it is possible to notice big fissures and cracks in all the samples. They were created by two main factors: (a) the transport of smaller particles toward the bottom by the infiltrating water and (b) the shrinking and swelling caused by the irrigations followed by drying time in the drying room.

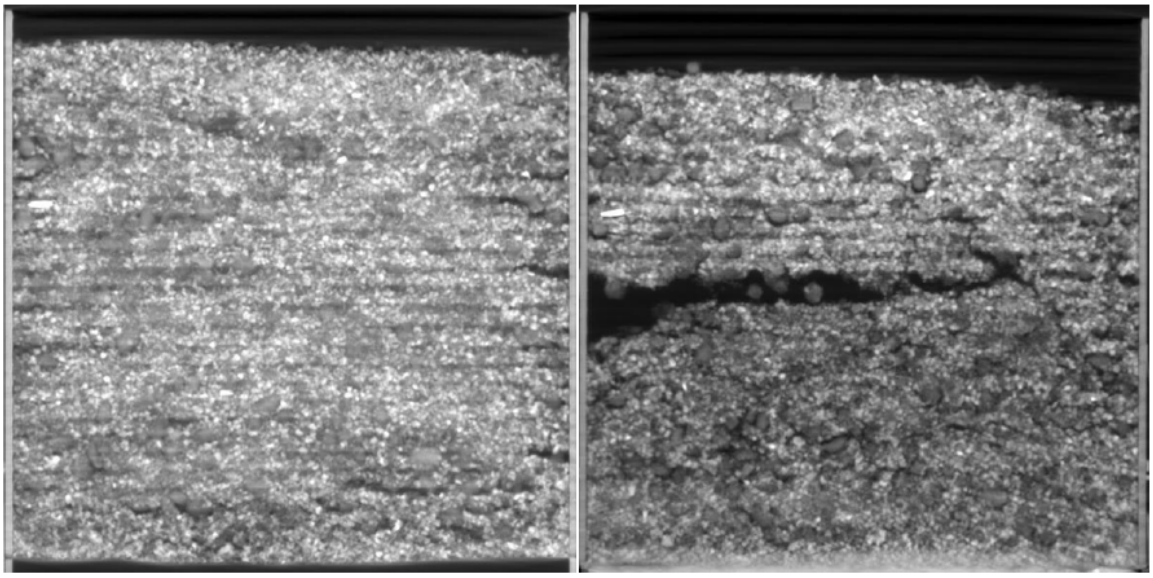

Figure 16: from the left: soil structure before the irrigations, soil structure after the irrigation (bare sample 2)

The same did not happen to the sown samples (Figure17) probably because, even though they went through the same exact procedure of the bare sample, they had the stabilizing effect of the plants root that prevented the creation of cracks and more time to consolidate. However, it is possible to notice that the smallest particles were transported by the water out of the sample as the grey scale has lower values in the after irrigation image.
As shown in Figure18 there were not major changes of the structure even in the garden soil samples. That is probably because: (a) stabilizing effect of plant roots, during the 4 weeks underground some plants grew in the boxes so, even though the amount of plants present in these samples was significantly lower than the one of the sown samples, the roots still had a small impact on the stabilization of the samples; (b) the smallest particles in the samples were already transported out of the boxes with rainfalls happened in the

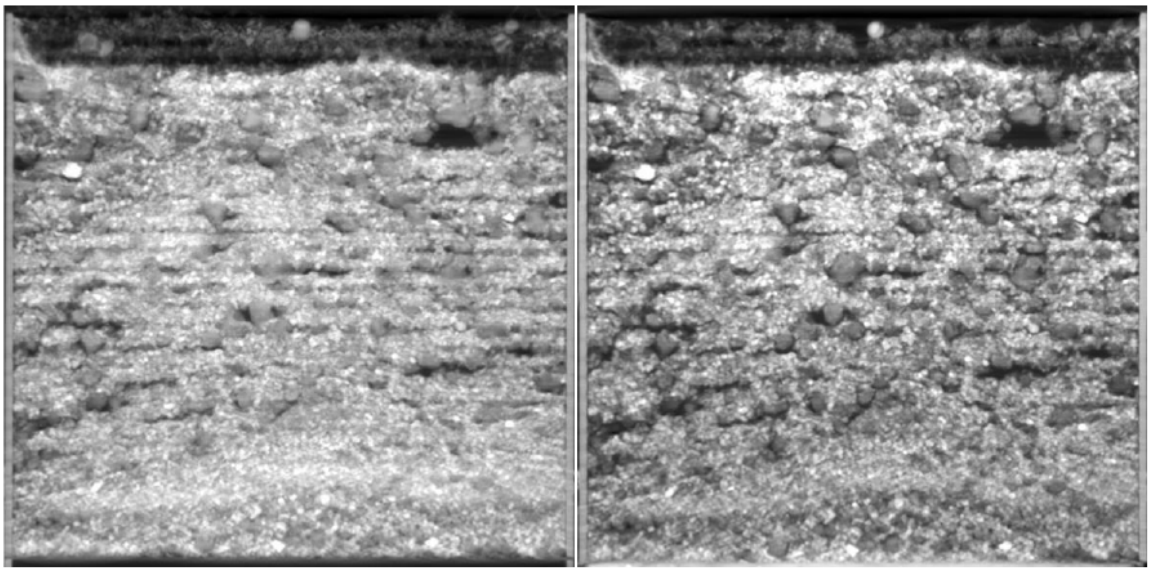

Figure 17: from the left: soil structure before the irrigations, soil structure after the irrigation (sown sample 3)

4 weeks time; (c) they had 4 weeks to consolidate.

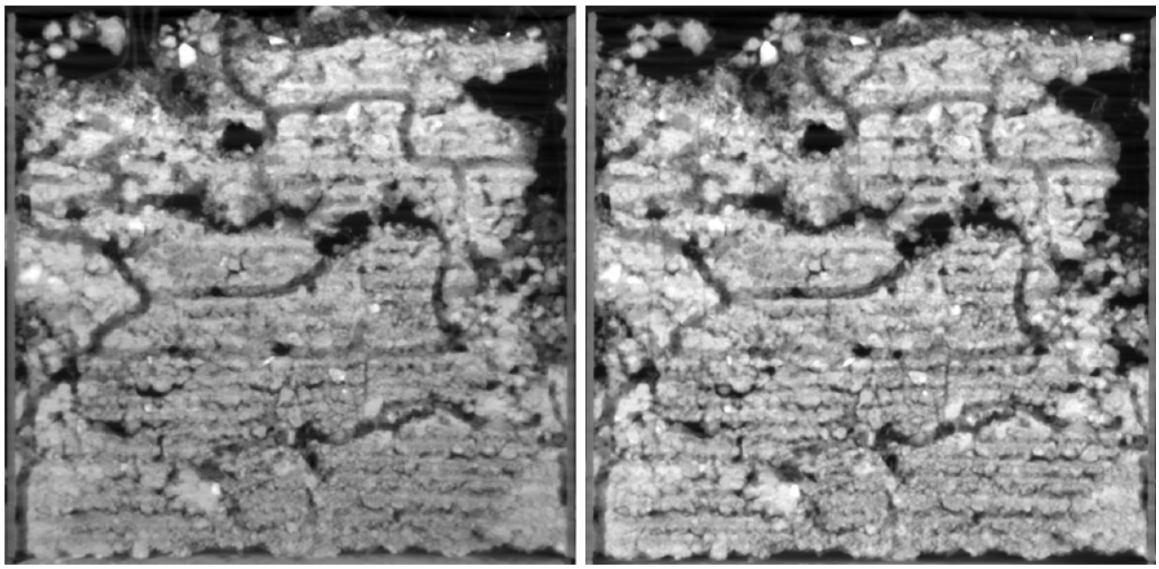

Figure 18: from the left: soil structure before the irrigations, soil structure after the irrigation (buried sample 3)

3.7 Weaknesses of the set up

An important downside of this experiment was the choice of the shape of the internal part of the boxes walls. The initial thought was that the ondulated shape would have decreased the water flow through the soil-box interface forcing the water to flow mainly

just through the soil, which it did. The problem with this shape is that it eased a lot the horizontal movement of water, making it easier for the wetting front to adsorb new fingers and making it impossible to do finger width related analysis which could have been an important outcome of the project.

Another disadvantage was that the samples were often slightly tilted, both in the x-direction and in the X-ray beam direction, because they were placed on a plastic tray that was not perfectly straight. The x-direction tilt probably eased preferential flow at one of the sides while the tilt in the X-ray direction eased the flow through the soil-box interface enhancing the problem previously discussed.

The biggest improvement that can be done is to modify the walls shape. The goal of this improvement would be to reduce the lateral movement caused by the current wall shape while keep reducing the flow through the soil-box interface. An idea could be to use a material that is naturally very rough and to merge the horizontal ondulated shape with a vertical ondulated shape.

4 Conclusions

In this study a laboratory experiment on preferential flow was conducted with the aim to quantify the importance of water repellency, soil structure and irrigation rate on water infiltration into soil.
The results of this experiment showed that:

- Water infiltration patterns through bare soil and garden soil (except garden soil sample 2) remained identical during different consecutive irrigation runs, we can therefore assume that if an irrigation leads to a certain infiltration pattern, the latter will be found after every irrigation done in the same soil and at the same rate;
- Water infiltration patterns trough soil with plants, unlike bare soils, are more likely to change with every irrigation event, even if irrigation rate and antecedent soil moisture are similar;
- Increasing the irrigation rate diminished the difference between the wetting front shapes of consecutive irrigation runs. It also reduced the wetting front tortuosity, i.e. preferential flow;
- There was a very good correlation between the tortuosity index trends and the wetting fronts. If, in the same sample at a certain time, all the tortosity index values are similar, even the wetting fronts will be similar;
- The tortosity of the wetting fronts increased with time;
- The four cases of possible water repellency reduced the water infiltration velocity through the soil of the 33.3%;
- The macroporosity was strongly related to the water infiltration velocity through soil. The bigger the macroporosity was the higher the water infiltration velocity;
- The water infiltration velocity through soil was influenced by the initial water content of the soil.
- Plants roots and long consolidation times exerted a stabilizing effect on the soil structure;

X-ray computed tomography demonstrated to be a useful technique to investigate water infiltration through the soil as was able to very well detect water in the soil samples. If used toghether with an image analysis software it has a huge potential as it can be used even for 3D infiltration experiments. The only limitation that it has is that there is a low maximum limit for the samples size, in fact the sample maximum width and height are respectively 50 and 60 cm. Furthermore, during this project, just a small part of the x-ray computed tomography potential has been used so to estimate its potential many more similar projects are needed.

With simple modifications to the set up it is possible to obtain important informations about the single fingers, like width, and not only of the wetting front.

Acknowledgement

First I want to thank John for giving me the opportunity to do this project, for helping me to conduct it and for patiently reviewing the manuscript.

I want to thank Daniel, whose help was fundamental for the realization of the project.

I want to thank Gloria Falsone, for accepting to be my italian supervisor and, therefore, allowing me to do my master thesis abroad.

I thank Anna Schwenk for letting me use the pump needed for this work.

The last thanks go to all the people that helped and supported me throughout the last two years and made all of this possible.

References

Baveye, P. C., Laba, M., Otten, W., Bouckaert, L., Sterpaio, P. D., Goswami, R. R., ... & Mooney, S. (2010). Observer-dependent variability of the thresholding step in the quantitative analysis of soil images and X-ray microtomography data. *Geoderma, 157*(1-2), 51-63.

Beven, K., & Germann, P. (1982). Macropores and water flow in soils. *Water resources research, 18*(5), 1311-1325.

Bughici, T., & Wallach, R. (2016). Formation of soil–water repellency in olive orchards and its influence on infiltration pattern. *Geoderma, 262*, 1-11.

Clothier, B. E., Green, S. R., & Deurer, M. (2008). Preferential flow and transport in soil: progress and prognosis. *European Journal of Soil Science, 59*(1), 2-13.

Cnudde, V., Boone, M. N. (2013). High-resolution X-ray computed tomography in geosciences: A review of the current technology and applications. *Earth-Science Reviews, 123*, 1-17.

Costanza, R., d'Arge, R., De Groot, R., Farber, S., Grasso, M., Hannon, B., ... & Raskin, R. G. (1997). The value of the world's ecosystem services and natural capital. *nature, 387*(6630), 253-260.

Cremer, C. J. M., Schuetz, C., Neuweiler, I., Lehmann, P., & Lehmann, E. H. (2017). Unstable Infiltration Experiments in Dry Porous Media. *Vadose Zone Journal, 16*(7).

DeBano, L. F. (1981). *Water repellent soils: a state-of-the-art* (Vol. 46). US Department of Agriculture, Forest Service, Pacific Southwest Forest and Range Experiment Station.

DeBano, L. F. (2000). The role of fire and soil heating on water repellency in wildland environments: a review. *Journal of hydrology, 231*, 195-206.

Dıaz-Zorita, M., Perfect, E., & Grove, J. H. (2002). Disruptive methods for assessing soil structure. *Soil and Tillage Research, 64*(1-2), 3-22.

Doerr, S. H., Shakesby, R. A., & Walsh, R. (2000). Soil water repellency: its causes, characteristics and hydro-geomorphological significance. *Earth-Science Reviews, 51*(1-4), 33-65.

Faybishenko, B. A. (1995). Hydraulic behavior of quasi-saturated soils in the presence of entrapped air: Laboratory experiments. *Water Resources Research, 31*(10), 2421-2435.

Flury, M., Flühler, H., Jury, W. A., & Leuenberger, J. (1994). Susceptibility of soils to preferential flow of water: A field study. *Water resources research, 30*(7), 1945-1954.

Fohrer, N., Berkenhagen, J., Hecker, J. M., & Rudolph, A. (1999). Changing soil and surface conditions during rainfall: single rainstorm/subsequent rainstorms. *Catena, 37*(3-4), 355-375.

Glass, R. J., & Steenhuis, T. S. (1984). Factors influencing infiltration flow instability and movement of toxics in layered sandy soils, Tech. Pap. 84-2508. *Am. Soc. of Agric. Eng., St. Joseph, Mich.*

Granovsky, A. V., McCoy, E. L., Dick, W. A., Shipitalo, M. J., & Edwards, W. M. (1994). Impacts of antecedant moisture and soil surface mulch coverage on water and chemical transport through a no-till soil. *Soil and Tillage Research, 32*(2-3), 223-236.

Gray, D. M., & Norum, D. I. (1967, November). The effect of soil moisture on infiltration as related to runoff and recharge. In *Proceedings of hydrology symposium* (No. 6).

Hardie, M. A., Cotching, W. E., Doyle, R. B., Holz, G., Lisson, S., & Mattern, K. (2011). Effect of antecedent soil moisture on preferential flow in a texture-contrast soil. *Journal of Hydrology, 398*(3-4), 191-201.

Hendrickx, J. M., & Flury, M. (2001). Uniform and preferential flow mechanisms in the vadose zone. *Conceptual models of flow and transport in the fractured vadose zone*, 149-187.

Hill, D. E., & Parlange, J. Y. (1972). Wetting front instability in layered soils. *Soil Science Society of America Journal, 36*(5), 697-702.

Hillel, D. (2003). *Introduction to environmental soil physics.* Elsevier.

Hubbert, K. R., Preisler, H. K., Wohlgemuth, P. M., Graham, R. C., & Narog, M. G. (2006). Prescribed burning effects on soil physical properties and soil water repellency in a steep chaparral watershed, southern California, USA. *Geoderma, 130*(3-4), 284-298.

Jarvis, N. J. (2007). A review of non-equilibrium water flow and solute transport in soil macropores: Principles, controlling factors and consequences for water quality. *European Journal of Soil Science, 58*(3), 523-546.

Jaynes, D. B., Ahmed, S. I., Kung, K. J., & Kanwar, R. S. (2001). Temporal dynamics of preferential flow to a subsurface drain. *Soil Science Society of America Journal, 65*(5), 1368-1376.

Koestel, J., & Schlüter, S. (2019). Quantification of the structure evolution in a garden soil over the course of two years. *Geoderma, 338*, 597-609.

Larsbo, M., Koestel, J., & Jarvis, N. (2014). Relations between macropore network characteristics and the degree of preferential solute transport. *Hydrology and Earth System Sciences, 18*(12), 5255-5269.

Leelamanie, D. A. L., Karube, J., & Yoshida, A. (2008). Characterizing water repellency indices: Contact angle and water drop penetration time of hydrophobized sand. *Soil Science & Plant Nutrition, 54*(2), 179-187.

Lili, M., Bralts, V. F., Yinghua, P., Han, L., & Tingwu, L. (2008). Methods for measuring soil infiltration: State of the art. *International Journal of Agricultural and Biological Engineering, 1*(1), 22-30.

Liu, Y., Steenhuis, T. S., & Parlange, J. Y. (1994). Formation and persistence of fingered flow fields in coarse grained soils under different moisture contents. *Journal of hydrology, 159*(1-4), 187-195.

Lucchese, L., & Mitra, S. K. (2001). Colour image segmentation: a state-of-the-art survey. *Proceedings-Indian National Science Academy Part A, 67*(2), 207-222.

MacDonald, L. H., & Huffman, E. L. (2004). Post-fire soil water repellency. *Soil Science Society of America Journal, 68*(5), 1729-1734.

Ogawa, S., Baveye, P., Boast, C. W., Parlange, J. Y., & Steenhuis, T. (1999). Surface fractal characteristics of preferential flow patterns in field soils: evaluation and effect of image processing. *Geoderma, 88*(3-4), 109-136.

Pagliai, M., Vignozzi, N., & Pellegrini, S. (2004). Soil structure and the effect of management practices. *Soil and Tillage Research, 79*(2), 131-143.

Parr, J. F., & Bertrand, A. R. (1960). Water infiltration into soils. In *Advances in Agronomy* (Vol. 12, pp. 311-363). Academic Press.

Rabot, E., Wiesmeier, M., Schlüter, S., & Vogel, H. J. (2018). Soil structure as an indicator of soil functions: a review. *Geoderma, 314*, 122-137.

Rezanezhad, F., Vogel, H. J., & Roth, K. (2006). Experimental study of fingered flow through initially dry sand.

Ridler, T. W., & Calvard, S. (1978). Picture thresholding using an iterative selection method. *IEEE trans syst Man Cybern, 8*(8), 630-632.

Ritsema, C. J., & Dekker, L. W. (1995). Distribution flow: A general process in the top layer of water repellent soils. *Water Resources Research, 31*(5), 1187-1200.

Rye, C. F., & Smettem, K. R. J. (2017). The effect of water repellent soil surface layers on preferential flow and bare soil evaporation. *Geoderma, 289*, 142-149.

Shipitalo, M. J., & Edwards, W. M. (1996). Effects of initial water content on macropore/matrix flow and transport of surface-applied chemicals. *Journal of Environmental Quality, 25*(4), 662-670.

Sililo, O. T., & Tellam, J. H. (2000). Fingering in unsaturated zone flow: a qualitative review with laboratory experiments on heterogeneous systems. *Groundwater, 38*(6), 864-871.

Snehota, M., Jelinkova, V., Sobotkova, M., Sacha, J., Vontobel, P., & Hovind, J. (2015). Water and entrapped air redistribution in heterogeneous sand sample: Quantitative neutron imaging of the process. *Water Resources Research, 51*(2), 1359-1371.

Wang, Y., Li, Y., Wang, X., & Chau, H. W. (2018). Finger flow development in layered water-repellent soils. *Vadose Zone Journal, 17*(1).

Wang, Z., Wu, Q. J., Wu, L., Ritsema, C. J., Dekker, L. W., & Feyen, J. (2000). Effects of soil water repellency on infiltration rate and flow instability. *Journal of Hydrology, 231*, 265-276.

Zlotnik, V. A., Eisenhauer, D. E., Schlautman, D. J., Zurbuchen, B. R., & Van Peursem, D. (2007). Entrapped air effects on dipole flow test in sand tank experiments: Hydraulic conductivity and head distribution. *Journal of hydrology, 339*(3-4), 193-205.